CAN WE EVER REACH THE HL-LHC REQUIREMENTS WITH THE INJECTORS?

H. Bartosik, T. Argyropoulos, B. Goddard, G. Iadarola, Y. Papaphilippou,
G. Rumolo, E. Shaposhnikova, CERN, Geneva, Switzerland

Abstract

The present intensity and brightness limitations of the LHC injector synchrotrons for 25 ns beams are space charge, beam loading, instabilities in the transverse and longitudinal planes and electron cloud effects. This paper reviews how these performance limitations are expected to change after implementing the mitigation measures foreseen within the Upgrade Scenario 2. The question is addressed whether the beam performance will match the requirements of the HL-LHC project. In particular, we assume operational scenarios with 25 ns beams produced with the traditional bunch splitting scheme in the PS and with the already tested batch compression scheme. A set of baseline parameters at LHC injection is then established based on extrapolation from the beam characteristics achieved in 2012 and the expected gains from the upgrades.

INTRODUCTION

The Upgrade Scenario 2 (US2) of the HL-LHC project aims at accumulating an integrated luminosity of 3000 fb^{-1} in p-p collisions at a center of mass energy of $\sqrt{s}=14$ TeV by the end of 2035. Reaching this goal requires an average integrated luminosity of 270 fb^{-1}/year during the HL-LHC era with levelling at an instantaneous luminosity of $5{\times}10^{34}$ cm^{-2}s^{-1} and the nominal 25 ns bunch spacing. The US2 baseline beam parameters at LHC injection are therefore targeted at an intensity of $N = 2.3\times10^{11}$ p/b within a normalized transverse emittance of $\varepsilon_n = 2.1\,\mu$m at LHC injection [1].

Before discussing the performance reach of the injector complex in US2, i.e. after the implementation of all upgrades planned within the LIU project, the operational beam characteristics achieved in 2012 shall be reviewed. Using the standard production scheme with 72 bunches per PS batch, the injectors delivered the 25 ns beam with about $N\approx1.2{\times}10^{11}$ p/b and transverse emittances of $\varepsilon_n\approx2.6\,\mu$m for the LHC Scrubbing Run. The successful implementation of the Batch Compression bunch Merging and Splitting (BCMS) scheme [2, 3] in the PS allowed reducing the number of splittings of each PSB bunch by a factor two at the expense of reducing the number of bunches per PS batch from 72 to 48. With this scheme a high brightness 25 ns beam with similar intensity per bunch but a transverse emittance of about $\varepsilon_n\approx1.4\,\mu$m at SPS extraction was provided to the LHC for the 25 ns pilot physics run. For both beam types, the achievable beam brightness is determined by the multi-turn injection in the PSB and space charge in the PS. The main intensity limitations for the 25 ns beams in the injector complex are due to electron cloud effects and longitudinal instabilities in the SPS. Stable beam conditions with four PS batches and bunch lengths at SPS extraction compatible with injection into the LHC were achieved for a maximum intensity of about $N\approx1.3\times10^{11}$ p/b.

Table 1: Beam loss and emittance growth budgets.

Machine	$-\Delta N/N_0$	$\Delta\varepsilon/\varepsilon_0$
PSB injection to extraction	5 %	5 %
PS injection to extraction	5 %	5 %
SPS injection to extraction	10 %	10 %
Total	19 %	21 %

For the following estimation of the achievable beam parameters out of the LHC injectors in the future, it is assumed that emittance growth and losses are both limited to 5 % in the PSB and in the PS, respectively, and to 10 % in the SPS as summarized in Table 1.

All upgrades for the PSB and PS foreseen in US2 are also part of Upgrade Scenario 1 (US1) and are discussed in more detail in Ref. [4]. The expected performance reach of the PS complex is therefore discussed only briefly in what follows. This paper is focused on the upgrades and measures, which aim at mitigating the performance limitations of the SPS.

PS COMPLEX

Space charge and beam brightness limitations

In the present configuration with LINAC2, the LHC beams are produced in the PSB at a constant beam brightness [5], which is mainly determined by the multi-turn injection process and space charge effects in the low energy part of the cycle. It is expected that the connection of LINAC4 and the H$^-$ charge exchange injection at 160 MeV will allow doubling the beam brightness out of the PSB [6], i.e. achieving twice the intensity for the same transverse emittance as compared to today's operation. This is illustrated in the limitation diagrams for the standard and the BCMS beam production schemes shown in Fig. 1, where the shaded areas correspond to beam parameters not accessible after the LIU upgrade. Note that the normalized transverse emittance is plotted as a function of the intensity per bunch at LHC injection (450 GeV) including already the budgets for emittance growth and losses through the injector chain as defined in Table 1.

In order to mitigate space charge effects on the PS injection plateau with the higher beam brightness available with

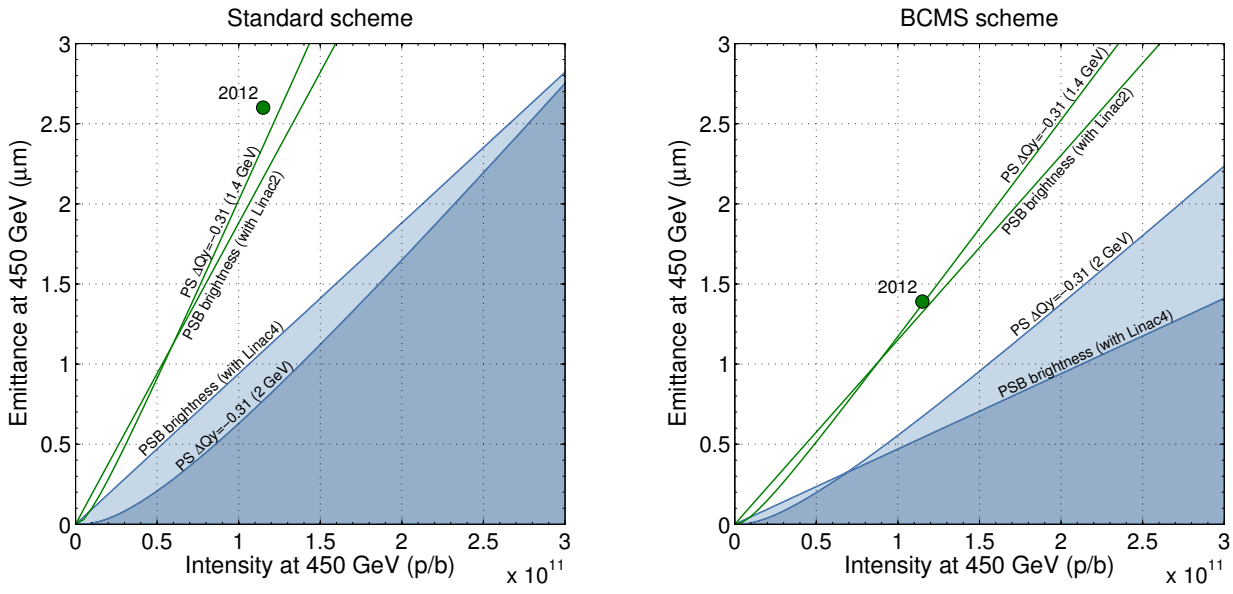

Figure 1: Beam brightness limitations in the PS complex for the standard 25 ns beam production scheme (left) and the 25 ns BCMS scheme (right) after the LIU upgrades (blue curves) and at present (green curves) together with the beam performance achieved in 2012 (green dots).

LINAC4, the PSB-PS transfer energy will be increased from the present 1.4 GeV to 2 GeV as part of the baseline LIU PSB and PS upgrades. Based on measurements with single bunch beams [7] and the operational experience with the high brightness 25 ns BCMS beam at 1.4 GeV, a maximum vertical space charge tune shift of $\Delta Q_y \approx -0.31$ on the PS injection plateau can be considered acceptable with respect to blow-up and losses [6]. The corresponding transverse emittance as a function of intensity per LHC bunch for this tune shift is shown in Fig. 1 together with the beam parameters at LHC injection achieved in 2012. The highest beam brightness in the PS achievable with the 2 GeV upgrade is then estimated assuming the maximum bunch length compatible with the PSB recombination kicker rise time, i.e. $\tau = 205$ ns for the standard production scheme (6 PSB bunches injected on harmonic number $h = 7$ in the PS) and $\tau = 135$ ns for the BCMS beams (8 PSB bunches injected on $h = 9$), and the largest longitudinal emittance compatible with the RF gymnastics. Note that after the implementation of the LIU upgrades, i.e. the connection of LINAC4 and the 2 GeV PSB-PS transfer, the PS complex is expected to deliver practically 25 ns beams with twice higher brightness as compared to the present performance.

Intensity limitations

Considering the operational experience with other high intensity beams, no intensity limitations from coherent beam instabilities are to be expected in the PSB within the parameter range of interest for HL-LHC

In the PS, longitudinal coupled-bunch instabilities during acceleration and at flat top presently limit the intensity of LHC beams to about $N \approx 1.9 \times 10^{11}$ p/b at extraction. Furthermore, transient beam loading induces asymmetries of the various bunch splittings and thus a bunch-to-bunch intensity variation along the bunch train. After the installation of a new coupled-bunch feedback system with a dedicated kicker cavity and new 1-turn delay feedback boards for beam loading compensation, the intensity limit will be pushed to more than $N = 2.5 \times 10^{11}$ p/b, beyond the requirement for the 25 ns HL-LHC beam [4].

Various instabilities in the transverse plane can be observed with LHC beams in the PS. Horizontal head-tail instabilities are encountered at flat bottom [8], which are presently cured by introducing linear coupling between the transverse planes and operating close to the coupling resonance. It was demonstrated in recent Machine Development (MD) studies that these head-tail instabilities at 1.4 GeV can be suppressed also by the PS transverse feedback system commissioned in 2012 [9], which has the advantage of providing additional flexibility for optimizing the machine working point for the space charge dominated LHC beams. The power amplifiers of this feedback are presently being upgraded in the frame of the LIU project in preparation for the future injection at 2 GeV.

The fast vertical instability observed in the PS during transition crossing with high intensity (TOF-like) beams is not expected to be a limitation for the HL-LHC beams [10]. However, a similar instability discovered recently with single bunch beams of small longitudinal emittance needs to be analyzed further in future MD studies, as it could not be cured with the aforementioned PS transverse feedback system due to its limited bandwidth [9].

After the final bunch splittings at the PS top energy re-

sulting in the 25 ns bunch spacing, an electron cloud is developing during the bunch shortening and bunch rotation before extraction to the SPS [11]. Nevertheless, no beam degradation has been observed so far in operational conditions as the time of interaction between the beam and the electron cloud is restricted to a few tens of milliseconds. It was observed in dedicated MD studies that the electron cloud drives a horizontal coupled bunch instability if the 25 ns beam is stored at top energy [12]. The onset time of this instability could be efficiently delayed by the PS transverse feedback system [9]. The electron cloud is therefore not expected to be a limitation for the HL-LHC beams.

SPS

The main challenges for future high intensity 25 ns LHC beams in the SPS are instabilities in the transverse and longitudinal planes, beam loading and RF power, electron cloud and space charge effects on the long injection plateau. Since the end of 2010, extensive machine studies have been performed with a low gamma transition optics. In comparison to the Q26 optics used in the past, which has 26 as the integer part of the betatron tunes and a gamma transition of $\gamma_t = 22.8$, the working point is lowered by 6 integer units in both planes in the Q20 optics [13] such that the transition energy is reduced to $\gamma_t = 18$. Consequently, the phase slip factor $\eta \equiv 1/\gamma_t^2 - 1/\gamma^2$ is increased throughout the acceleration cycle with the largest relative gain of a factor 3 at injection energy, as illustrated in Fig. 2. As the

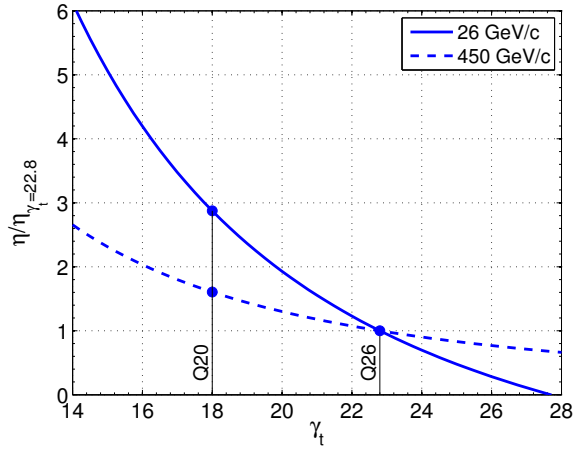

Figure 2: Phase slip factor η relative to the value of the Q26 SPS optics as a function of the gamma transition. The values of $\gamma_t = 22.8$ and $\gamma_t = 18$ correspond to the Q26 and Q20 optics, respectively.

intensity thresholds for all instabilities observed in the SPS scale with the slip factor η, a significant improvement of beam stability is achieved with the Q20 optics as discussed in more detail below. The Q20 optics is being used successfully in routine operation for LHC filling since September 2012 [14] and will be the default machine configuration for LHC beams in the SPS in the future.

Transverse Mode Coupling Instability

The vertical single bunch Transverse Mode Coupling Instability (TMCI) at injection is one of the main intensity limitations in the Q26 optics. For bunches injected with the nominal longitudinal emittance $\varepsilon_l = 0.35$ eVs, the corresponding instability threshold is around $N_{th} \approx 1.6{\times}10^{11}$ p/b (with vertical chromaticity close to zero) [15]. The instability results in emittance blow-up and fast losses as shown in Fig. 3 (top). Slightly higher intensities can be reached when increasing the chromaticity, however at the expense of enhanced incoherent emittance growth and losses on the flat bottom.

Analytical models based on a broadband impedance predict that the instability threshold with zero chromaticity scales like $N_{th} \propto |\eta|\varepsilon_l/\beta_y$ [16], where β_y denotes the vertical beta function at the location of the impedance source. Thus, the instability threshold can be raised by injecting bunches with larger longitudinal emittance. However, the

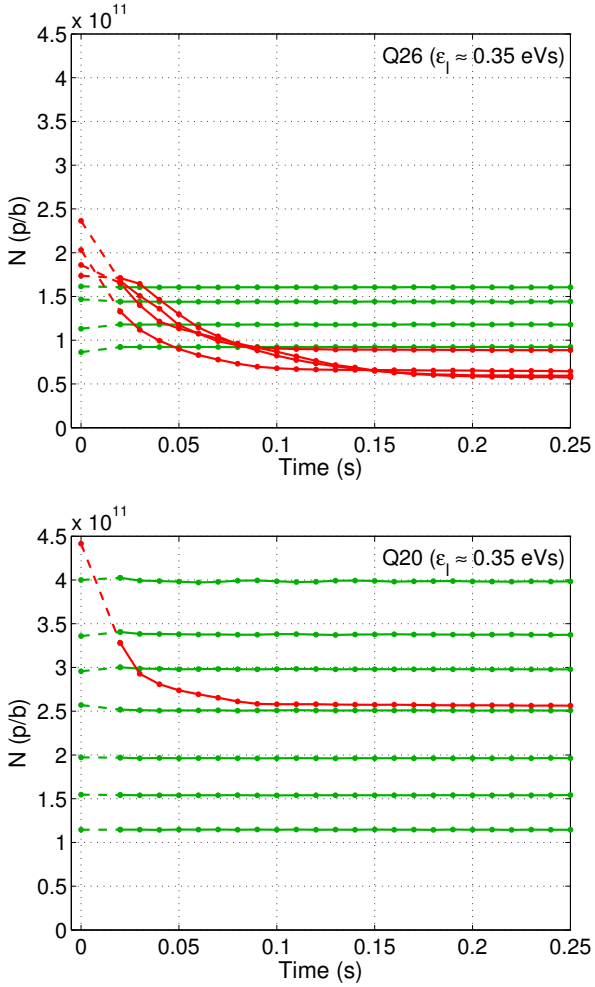

Figure 3: Examples of the intensity evolution as a function of time after injection in the Q26 optics (top) and the Q20 optics (bottom). Green curves correspond to stable beam conditions, red traces indicate cases above the TMCI threshold.

beam transmission between PS and SPS is degrading for larger longitudinal emittances unless additional cavities in the PS are used for optimizing the bunch rotation at extraction [17]. On the other hand, a significant increase of the instability threshold is expected in the Q20 optics even with the nominal longitudinal emittance, since the product of the slip factor and the vertical beta function at important impedance sources ($\eta\,\beta_y$) is about 2.5 times higher compared to the Q26 optics. This has been verified in measurements with high intensity single bunch beams as shown in Fig. 3 (bottom). The instability threshold in the Q20 optics for chromaticity close to zero and nominal longitudinal emittance was found at around $N_{th} \approx 4.5\times10^{11}$ p/b in good agreement with numerical simulations using the latest SPS impedance model [18].

With the Q20 optics the TMCI is not of concern for the beam parameters envisaged by the HL-LHC, even for the 50 ns "back-up" scenario [19] which requires significantly higher intensities per bunch compared to the 25 ns beams.

Space charge

After the successful implementation of the BCMS scheme [3], the PS was able to provide a high brightness 50 ns beam with an intensity of $N \approx 1.95\times10^{11}$ p/b and transverse emittances of about $\varepsilon_n \approx 1.1\,\mu$m at the end of 2012. A working point scan was performed with the Q20 optics using this beam in order to see how much space in the tune diagram is needed to accommodate the incoherent space charge tune spread and thus to minimize emittance blow-up. For each working point, the transverse emittances were measured with the wire scanners in turn acquisition mode (average profile along the bunch train) at the end of the 10.8 s flat bottom of the LHC cycle. Single batches were used for this experiment in order to study the blow-up along the entire injection plateau.

Figure 4 shows the measured transverse emittances for vertical tunes between $Q_y = 20.08$ and $Q_y = 20.23$ and a horizontal tune of about $Q_x \approx 20.13$, where the error bars indicate the spread over several measurements. Significant emittance blow-up is observed for vertical tunes close to the integer resonance, while the sum of the two transverse emittances is preserved for vertical tunes above $Q_y = 20.19$. This is consistent with the calculated incoherent space charge tune spread of $\Delta Q_x = -0.11$ and $\Delta Q_y = -0.20$ for a bunch length of $\tau \approx 3$ ns and an rms momentum spread of $\delta p/p_0 \approx 1.5\times10^{-3}$. For all the working points studied here, the losses on the injection plateau were typically of the order of 1% and the total transmission up to flat top was usually about 93% (without scraping). Further details are given in Ref. [20].

Based on the above results and considering the budgets for emittance blow-up and losses defined in Table 1, which permit slightly more blow-up in the SPS than observed in the measurements, the presently maximum acceptable space charge tune shift in the SPS for an optimized working point is set to $\Delta Q_y = -0.21$.

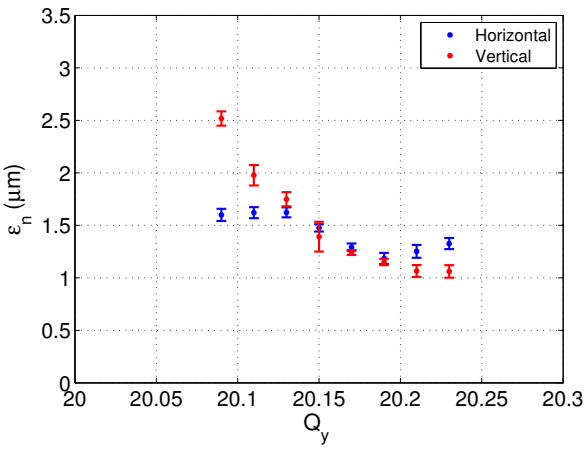

Figure 4: Transverse emittances measured at the end of the flat bottom as a function of the vertical tune. Measurements performed with single batches of the 50 ns BCMS beam.

Longitudinal instabilities and RF power

The longitudinal instabilities observed with LHC beams in the SPS are a combination of single bunch and coupled bunch effects [21]. The beam is stabilized in routine operation by increasing the synchrotron frequency spread using the 4th harmonic (800 MHz) RF system in bunch-shortening mode in combination with controlled longitudinal emittance blow-up along the ramp, which is performed with band-limited phase noise in the main 200 MHz RF system.

For a given longitudinal emittance and matched RF voltage the thresholds of the longitudinal coupled bunch instability and the single bunch instability due to loss of Landau damping scale proportional to the slip factor η [22]. Improved longitudinal beam stability was therefore observed in measurements with the Q20 optics at injection and during the ramp [23], where sufficient RF voltage is available to restore the same bucket area as with the Q26 optics. In fact, the Q20 optics provides significant margin for increasing the beam intensity at injection energy, where the attainable longitudinal emittance is limited by capture losses and the transfer efficiency between the PS and SPS.

The situation is different at flat top. The maximum voltage is applied in both optics in order to shorten the bunches for the transfer into the 400 MHz buckets of the LHC. Better beam stability would still be achieved in the Q20 optics for a given longitudinal emittance, however, in this case the bunches would be longer. In order to have the same bunch length in the two optics, the longitudinal emittance thus has to be smaller in the Q20 optics. From the scaling of the instability threshold for loss of Landau damping (LD) [22] it follows that the same beam stability is obtained in both optics for the same bunch length at extraction.

At the end of 2012, a series of MD sessions were devoted to the study of high intensity 25 ns beams in the Q20 optics. Figure 5 shows the measurements of the bunch length along

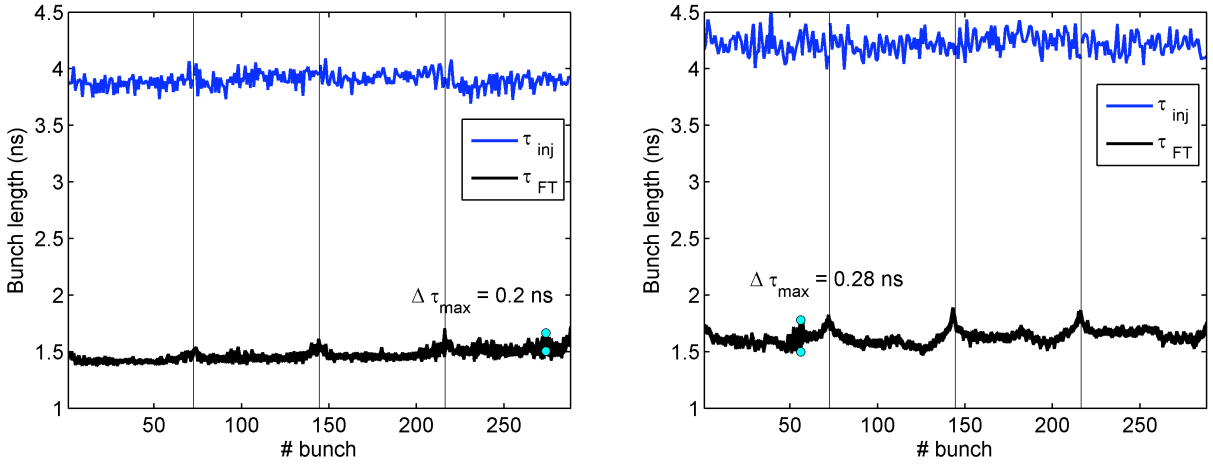

Figure 5: Bunch length measurements along the four batches of the 25 ns beam in the Q20 optics for intensities of about $N \approx 1.2\times10^{11}$ p/b (left) and $N \approx 1.35\times10^{11}$ p/b (right). The blue trace corresponds to injection and the black traces correspond to 8 measurements within one synchrotron period at flat top. The maximum bunch length variation $\Delta\tau_{\max}$ due to quadrupole oscillations at flat top is indicated.

the train at injection and at flat top for two different intensities. Note that the average bunch length increases by about 10% when pushing the intensity from $N\approx1.2\times10^{11}$ p/b to $N\approx1.35\times10^{11}$ p/b. The reason for that is the larger longitudinal emittance of the beam already at injection (bunches are already longer) and the controlled longitudinal emittance blow-up in the SPS required for beam stabilization. The intensity of $N\approx1.35\times10^{11}$ p/b is considered to be the maximum intensity reachable with the present RF system in the SPS, since the average bunch length of $\tau \approx 1.65$ ns achieved with this intensity is close to the maximum acceptable for transfer to the LHC. For higher beam intensities, larger RF voltage is needed in order to maintain the same bunch length with the increased longitudinal emittance required for beam stability. Using the scaling law for single bunch instability due to loss of Landau damping, the RF voltage needs to be increased proportional to the intensity [24].

The 200 MHz main RF system of the SPS consists of four travelling wave cavities [25], of which two are made of four sections and the other two are made of five sections. The maximum RF power presently available in continuos mode is about 0.75 MW per cavity, which corresponds to a maximum total RF voltage of about 7.5 MV at nominal intensity of the 25 ns beam. However, less RF voltage is available for higher beam intensity due to the effect of beam loading and the limited RF power [26]. This voltage reduction is larger for longer cavities, i.e. it is increasing with the number of cavity sections. The LIU baseline upgrades for the SPS include an upgrade of the low-level RF and a major upgrade of the 200 MHz RF system [27]. The low-level RF upgrade, which is also part of US1 [4], will allow pulsing the RF amplifiers with the revolution frequency (the LHC beam occupies less than half of the SPS circumference) leading to an increase of the RF power up to about 1.05 MW per cavity. The main upgrade consists of the rearrangement of the four existing cavities and two spare sections into two 4-section cavities and four 3-section cavities, and the construction of two additional power plants providing 1.6 MW each. This will entail a reduction of the beam loading per cavity, an increase of the available RF voltage and a reduction of the beam coupling impedance (the peak value at the fundamental frequency).

Figure 6 shows the maximum total RF voltage of the SPS 200 MHz system as a function of the beam current with and without the RF upgrades. The RF voltage required for keeping the bunch length constant with increasing inten-

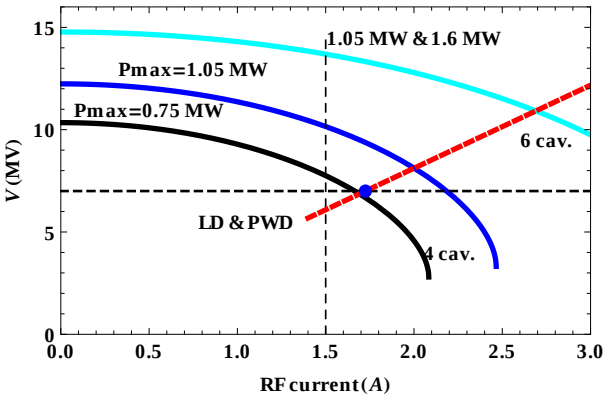

Figure 6: Maximum total RF voltage as a function of the beam current for different cases: present situation (black line), after the low-level RF upgrade to operate in pulsed mode (blue line) and after the cavity rearrangement and the construction of two additional power plants of 1.6 MW each (light blue line). The voltage required for maintaining constant bunch length at extraction taking into account the single bunch longitudinal instability and the voltage reduction due to potential well distortion is also shown (red dashed line) together with the reference point (blue dot).

sity taking into account the compensation of potential well distortion (PWD) and the required longitudinal emittance blow-up for stabilizing the beam against the single bunch instability (loss of Landau damping) is indicated in the same graph. The presently maximum achieved intensity of $N \approx 1.35 \times 10^{11}$ p/b (corresponding to 1.7 A beam current) together with the corresponding maximum RF voltage of 7 MV serves as reference point. It follows that a maximum beam current of 1.9 A will be in reach after the low-level upgrade (4 times 1.05 MW pulsed) and 2.7 A after the full RF upgrade (cavities rearranged into six with 4×1.05 MW and 2×1.6 MW) [24]. These values correspond to maximum intensities at extraction of about $N \approx 1.45 \times 10^{11}$ p/b and $N \approx 2.0 \times 10^{11}$ p/b, respectively, when taking into account 3% intensity reduction due to scraping before extraction for cleaning transverse beam tails. However it should be emphasized that this estimation is based on simplified scaling laws and that slightly longer bunches, if accepted by the LHC, are significantly more stable ($\sim \tau^5$).

Electron cloud

The electron cloud effect has been identified as a possible performance limitation for the SPS since LHC type beams with 25 ns spacing were injected into the machine for the first time in the early years of 2000. At that time a severe pressure rise was observed all around the machine together with transverse beam instabilities, important losses and emittance blow-up on the trailing bunches of the train [28]. Since 2002, Scrubbing Runs with 25 ns beams were carried out almost every year of operation in order to condition the inner surfaces of the vacuum chambers and therefore mitigate the electron cloud. This allowed achieving a good conditioning state of the SPS up to 2012, both in terms of dynamic pressure rise and beam quality. During the Scrubbing Run of the LHC at the end of 2012, the 25 ns beam was regularly extracted from the SPS Q20 optics with four batches of 72 bunches with $N \approx 1.2 \times 10^{11}$ p/b and normalized transverse emittances of about 2.6 μm [14]. Extensive machine studies showed that for this beam intensity the 2012 conditioning state of the SPS is sufficient for suppressing any possible beam degradation due to electron cloud on the cycle timescale [29].

Further experiments performed with the Q20 optics showed that it was possible to inject the full train of the 25 ns beam with up to $N \approx 1.35 \times 10^{11}$ p/b without transverse emittance blow-up and preserve the beam quality up to extraction energy, as shown in Fig. 7 (top). For higher intensities ($N \approx 1.45 \times 10^{11}$ p/b injected) a transverse instability was observed after the injection of the third and the fourth batch, leading to emittance blow up as shown in Fig. 7 (bottom) and particle losses on the trailing bunches of the injected trains. The observed pattern on the bunch by bunch emittance is typical for electron cloud effects. Since the SPS was never scrubbed with such high beam intensities, an additional scrubbing step might be required for suppressing these effects.

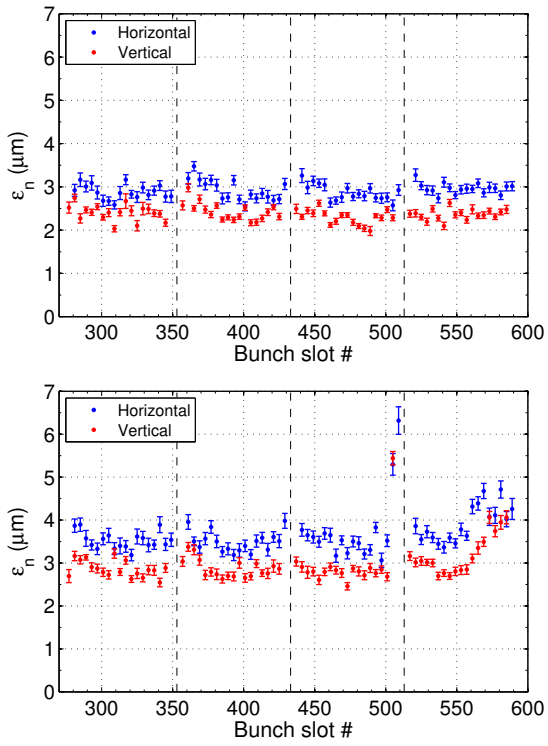

Figure 7: Bunch by bunch emittances measured at the SPS flat top for 4×72 bunches of the 25 ns LHC beam with intensities at injection of $N \approx 1.35 \times 10^{11}$ p/b (top) and $N \approx 1.45 \times 10^{11}$ p/b (bottom).

Several studies have been devoted in 2012 to the optimization of the scrubbing process and in particular to the definition and test of a possible "scrubbing beam", i.e. a beam produced specifically for scrubbing purposes, providing a higher scrubbing efficiency compared to the standard LHC type 25 ns beam. A 25 ns spaced train of "doublets", each of these consisting of two 5 ns spaced bunches, has been proposed [30]. As shown in simulations, this beam has indeed a lower multipacting threshold compared to the standard 25 ns beam due to the shorter empty gap between subsequent doublets, which enhances the accumulation of electrons in the vacuum chamber. For producing this beam with the existing RF systems of the injectors, long bunches from the PS ($\tau \approx 10$ ns full length) have to be injected into the SPS on the unstable phase of the 200 MHz RF system and captured in two neighboring buckets by raising the voltage within the first few milliseconds. Very good capture efficiency (above 90%) could be achieved for intensities up to 1.7×10^{11} p/doublet.

Figure 8 (top) shows the evolution of the longitudinal profile of the beam during the "splitting" right after the injection in the SPS. Figure 8 (bottom) shows the "final" beam profile, measured one second after injection. It was also verified that it is possible to rapidly lower the RF voltage and inject a second train from the PS without any important degradation of the circulating beam. Observations on the dynamic pressure rise in the SPS arcs confirmed

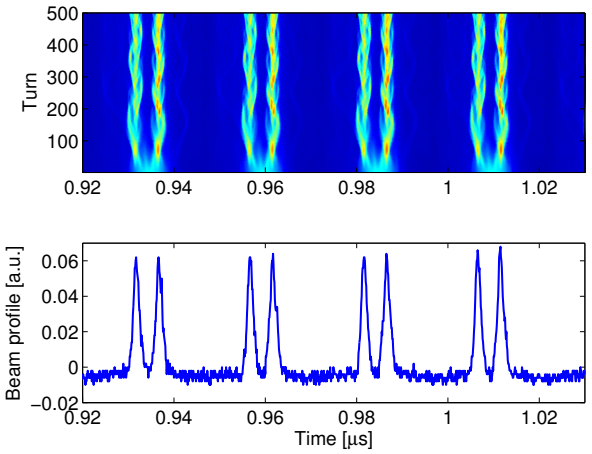

Figure 8: Evolution of the longitudinal beam profile in the SPS during the splitting at injection for the production of the doublet beam (top) and longitudinal bunch profiles of the doublet beam measured 1 s after injection (bottom).

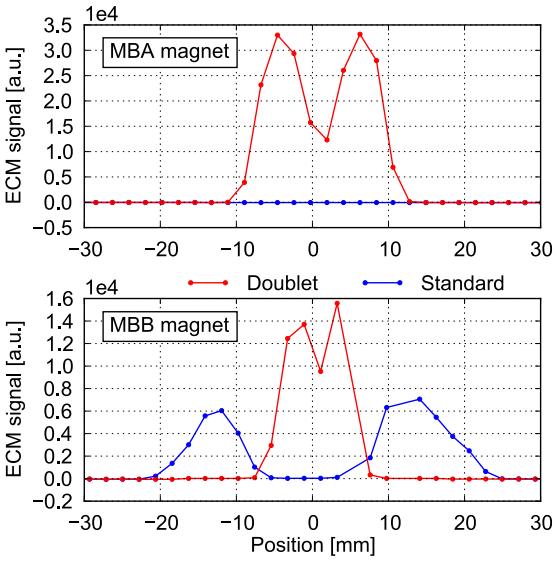

Figure 9: Electron cloud profiles measured in the strip detectors with MBA (top) and MBB (bottom) chambers with the standard 25 ns beam and with the doublet beam (same total intensity, 72 bunches from the PS with $N \approx 1.65 \times 10^{11}$ p/b).

the enhancement of the electron cloud activity as expected from simulations. The enhancement was also observed with the dedicated SPS strip detectors as shown in Fig. 9 for the two SPS vacuum chamber types, MBA and MBB, where the electron cloud profiles measured with the standard 25 ns beam and with the doublet beam are compared for the same total intensity. In this experiment with a single batch from the PS, electron cloud formation in the MBA is only observed with the doublet beam due to its lower multipacting threshold compared to the standard beam. In the MBB, where the nominal beam was still able to produce electron cloud, a clear enhancement of the peak electron density can be observed. It is important to note that the electron cloud produced by the doublets does not cover the full region to be conditioned for the standard beam. Therefore it is necessary to periodically displace the beam (using radial steering and orbit correction dipoles) during the scrubbing in order to achieve a satisfactory conditioning across the chamber surface.

A high bandwidth (intra-bunch) transverse feedback system is being developed for the SPS as part of the LIU project in collaboration with the LHC Accelerator Research Program (LARP), with the goal of fighting electron cloud instabilities and improving the beam quality during the scrubbing for making it more efficient. In 2013, experimental studies with prototype hardware already demonstrated the successful suppression of slow headtail instabilities of mode 0 (dipole mode) with single bunches. Further studies with improved hardware will follow in 2014.

In case scrubbing is not sufficient for suppressing the electron cloud effect with the high beam intensity and small transverse emittance required for HL-LHC, or in case the reconditioning process is very slow after large parts of the machine are vented (like during a long shutdown), the inner surface of the SPS vacuum chambers has to be coated with a low SEY material. The solution developed at CERN is to produce a thin film of amorphous Carbon using DC Hollow Cathode sputtering directly inside the vacuum chamber [31]. The suppression of electron cloud in coated prototype vacuum chambers has been fully validated with beam in the SPS [29]. Additional four SPS half cells (including quadrupoles) coated with amorphous Carbon will be ready for the startup in 2014 for further tests with beam.

The coating of the entire machine circumference of the SPS with amorphous Carbon is a major work, which requires careful preparation and planning of resources (as all magnets need to be transported to a workshop). The decision if the SPS needs to be coated or if scrubbing as electron cloud mitigation is sufficient has therefore to be taken not later than mid 2015. After the long shutdown, a Scrubbing Run of about two weeks will be performed during the startup at the end of 2014 with the goal of recovering the operational performance, as it is expected that the good conditioning state of the SPS will be degraded due to the long period without beam operation and the related interventions on the machine. Another Scrubbing Run will be performed in the first half of 2015 in order to scrub the machine for high intensity 25 ns beams. The final decision about the coating will be based on the experience during this period and on the outcome of experimental studies with the high intensity 25 ns beams.

INJECTORS PERFORMANCE REACH

The expected performance reach of the entire LHC injector chain after implementation of the LIU upgrades is shown in Fig. 10 for the standard and the BCMS scheme. The beam parameters are given at LHC injection taking

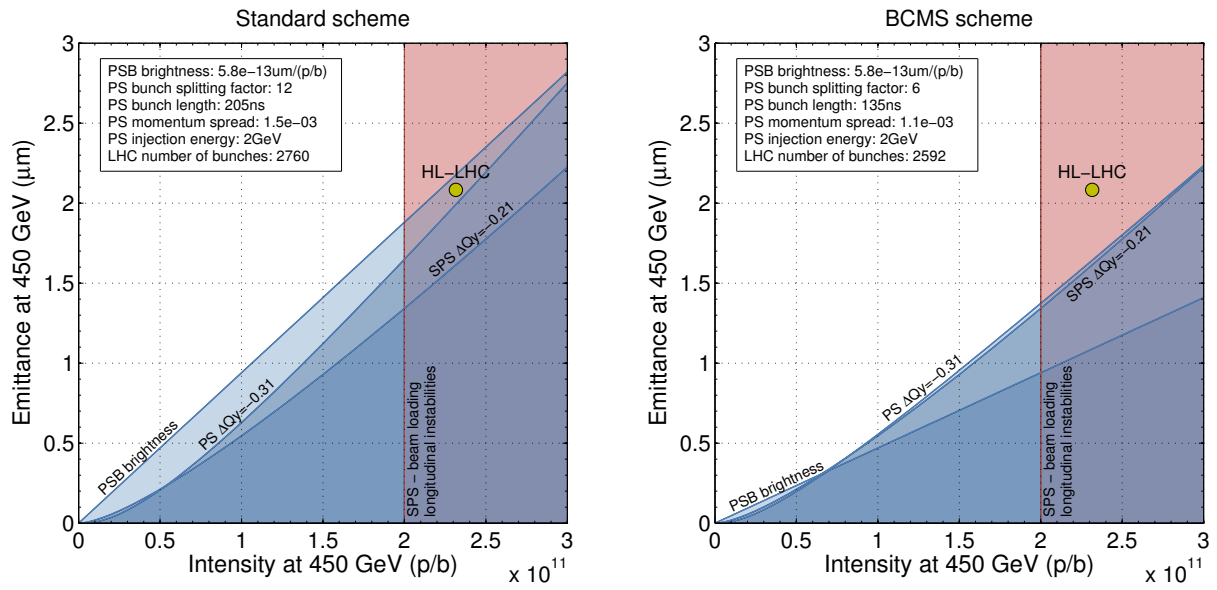

Figure 10: Limitation diagrams for 25 ns beams produced with the standard scheme (left) and the BCMS scheme (right) after implementation of the LIU upgrades.

Table 2: Achievable beam parameters after implementation of LIU upgrades in comparison with HL-LHC request.

		PSB						
		N (10^{11} p)	$\epsilon_{x,y}$ (μm)	E (GeV)	ϵ_z (eVs)	B_l (ns)	$\delta p/p_0$	$\Delta Q_{x,y}$
LIU-US2	Standard	29.55	1.55	0.16	1.4	650	$1.8 \cdot 10^{-3}$	(0.55, 0.66)
	BCMS	14.77	1.13	0.16	1.4	650	$1.8 \cdot 10^{-3}$	(0.35, 0.44)
HL-LHC		34.21	1.72	0.16	1.4	650	$1.8 \cdot 10^{-3}$	(0.58, 0.69)

		PS (double injection)						
		N (10^{11} p/b)	$\epsilon_{x,y}$ (μm)	E (GeV)	ϵ_z (eVs/b)	B_l (ns)	$\delta p/p_0$	$\Delta Q_{x,y}$
LIU-US2	Standard	28.07	1.63	2.0	3.00	205	$1.5 \cdot 10^{-3}$	(0.16, 0.28)
	BCMS	14.04	1.19	2.0	1.48	135	$1.1 \cdot 10^{-3}$	(0.19, 0.31)
HL-LHC		32.50	1.80	2.0	3.00	205	$1.5 \cdot 10^{-3}$	(0.18, 0.30)

		SPS (several injections)						
		N (10^{11} p/b)	$\epsilon_{x,y}$ (μm)	p (GeV/c)	ϵ_z (eVs/b)	B_l (ns)	$\delta p/p_0$	$\Delta Q_{x,y}$
LIU-US2	Standard	2.22	1.71	26	0.42	3.0	$1.5 \cdot 10^{-3}$	(0.09, 0.16)
	BCMS	2.22	1.25	26	0.42	3.0	$1.5 \cdot 10^{-3}$	(0.12, 0.21)
HL-LHC		2.57	1.89	26	0.42	3.0	$1.5 \cdot 10^{-3}$	(0.10, 0.17)

		LHC					
		N (10^{11} p/b)	$\epsilon_{x,y}$ (μm)	p (GeV/c)	ϵ_z (eVs/b)	B_l (ns)	bunches/train
LIU-US2	Standard	2.00	1.88	450	0.60	1.65	72
	BCMS	2.00	1.37	450	0.60	1.65	48
HL-LHC		2.32	2.08	450	0.65	1.65	72

into account the emittance growth and loss budgets from Table 1. The shaded areas correspond to regions in the parameter space that cannot be accessed. The best beam parameters correspond to an intensity of $N = 2.0 \times 10^{11}$ p/b (limited by longitudinal instabilities and RF power in the SPS) within transverse emittances of $\varepsilon_n = 1.88\,\mu$m for the standard scheme (limited by the PSB brigthness) and $\varepsilon_n = 1.37\,\mu$m for the BCMS scheme (limited by space charge in the PS and SPS), as summarized in Table 2. Although the beam parameters do not match the HL-LHC 'point-like' request (in particular the intensity per bunch), the injectors performance will be enough to saturate the LHC performance for the assumed pile-up limit and availability/fill length [1].

SUMMARY AND CONCLUSIONS

The connection of LINAC4 will double the beam brightness out of the PSB compared to the present operation, thanks to the H^- charge exchange injection and the higher injection energy of 160 MeV. Raising the PS injection energy to 2 GeV will mitigate space charge effects on the injection plateau and match the performance of the PS to the higher brightness available with LINAC4. The upgrades of the transverse and longitudinal feedbacks in the PS together with the RF upgrades will push present intensity limits beyond the requirements for HL-HLC. With the SPS Q20 optics the TMCI at injection is not an issue. The major SPS RF upgrade with two new power plants and rearranged RF cavities will push the achievable intensity from the present $N = 1.3 \times 10^{11}$ p/b to $N = 2.0 \times 10^{11}$ p/b. The decision if the SPS vacuum chambers all around the machine will be coated with amorphous Carbon in order to suppress the electron cloud will be taken in mid 2015 based on the experience and experimental studies from two Scrubbing Runs to be performed in 2014 and 2015. The main question is if scrubbing (for example with the doublet scrubbing beam) as electron cloud mitigation instead of the coating is a viable path for recovering the operational performance after a long shutdown and if the electron cloud can be suppressed for the future high intensity beams.

The overall performance of the LHC injectors after the implementation of all baseline LIU upgrades, i.e. an intensity of $N = 2.0 \times 10^{11}$ p/b and a transverse emittance of $\varepsilon_n = 1.88\,\mu$m for the 25 ns beam with 72 bunches per PS batch (standard scheme), approximately matches the parameters needed by HL-LHC with the presently assumed pile-up limit and machine physics efficiency. For achieving this performance, all upgrades must be effective, i.e. also those not explicitly mentioned in this paper but important for eliminating operational limitations or assuring reliability of the complex. Unless slightly longer bunches can be accepted by the LHC, there is little or no margin to further increase the intensity per bunch extracted from the SPS, as longitudinal instabilities in combination with beam loading will limit the maximum intensity even after the major RF upgrade of the SPS.

ACKNOWLEDGEMENTS

The authors would like to thank J. Bauche, T. Bohl, K. Cornelis, P. Costa Pinto, H. Damerau, R. de Maria, J. Esteban Müller, R. Garoby, S. Gilardoni, S. Hancock, W. Höfle, M. Meddahi, B. Mikulec, M. Taborelli, H. Timko and R. Wasef for support and helpful discussion.

REFERENCES

[1] R. de Maria *et al.*, "How to maximize the HL-LHC performance?", these proceedings.

[2] R. Garoby, "New RF Exercises Envisaged in the CERN-PS for the Antiprotons Production Beam of the ACOL Machine", IEEE Transactions on Nuclear Science, Vol. NS-32., No. 5 (1985).

[3] H. Damerau *et al.*, "RF manipulations for higher beam brightness LHC-type beams", CERN-ACC-2013-0210.

[4] S. Gilardoni *et al.*, "LIU: Which beams in the injectors fulfil HL-LHC Upgrade Scenario 1 goals?", these proceedings.

[5] B. Mikulec *et al.*, "Performance reach of LHC beams", in LIU Beam Studies Review, CERN (2012).

[6] G. Rumolo *et al.*, "Expected performance in the injectors at 25 ns without and with LINAC4", these proceedings.

[7] R. Wasef *et al.*, "Space Charge Effects and Limitations in the CERN Proton Synchrotron", CERN-ACC-2013-0176.

[8] R. Cappi, "Observation of high-order head-tail instabilities at the CERN-PS", CERN-PS-95-02-PA.

[9] G. Sterbini *et al.*, "Beam Tests and Plans for the Cern PS Transverse Damper System", CERN-ACC-2013-0215.

[10] S. Aumon, "High Intensity Beam Issues in the CERN Proton Synchrotron", CERN-THESIS-2012-261, PhD. thesis (2012).

[11] G. Iadarola *et al.*, "Electron Cloud Studies for the Upgrade of the CERN PS", CERN-ACC-2013-0095.

[12] R. Cappi *et al.*, "Electron cloud buildup and related instability in the CERN Proton Synchrotron", PRST-AB 5, 094401 (2002).

[13] H. Bartosik *et al.*, "Optics considerations for lowering transition energy in the SPS", CERN-ATS-2011-088.

[14] Y. Papaphilippou *et al.*, "Operational performance of the LHC proton beams with the SPS low transition optics", CERN-ACC-2013-0124.

[15] B. Salvant *et al.*, "Probing intensity limits of LHC-Type bunches in CERN SPS with nominal optics", CERN-ATS-2011-176.

[16] E. Métral, "Overview of Single-Beam Coherent Instabilities in Circular Accelerators", Proceedings of the 1st CARE-HHH-APD Workshop on Beam Dynamics in Future Hadron Colliders and Rapidly Cycling High-Intensity Synchrotrons, Geneva, Switzerland (2004).

[17] H. Timko *et al.*, "Experimental and simulation studies of the PS-to-SPS beam transfer efficiency", CERN-ATS-Note-2012-059 PERF.

[18] H. Bartosik, "Beam dynamics and optics studies for the LHC injectors upgrade", CERN-THESIS-2013-257, PhD. thesis (2013).

[19] V. Kain *et al.*, "50 ns back-up scenario", these proceedings.

[20] H. Bartosik *et al.*, "Experimental Studies for Future LHC Beams in the SPS", CERN-ACC-2013-0151.

[21] E. Shaposhnikova *et al.*, "Longitudinal Instabilities in the SPS and Beam Dynamics Issues with High Harmonic RF Systems", Proceedings of HB2012, Beijing, China (2012).

[22] E. Shaposhnikova, "Longitudinal stability of the LHC beam in the SPS", SL-Note-2001-031-HRF.

[23] H. Bartosik *et al.*, "Experimental studies with low transition energy optics in the SPS", CERN-ATS-2011-086.

[24] E. Shaposhnikova, "SPS intensity limitation with and without 200 MHz RF upgrade", presentation in the LIU SPS-Beam Dynamics Working Group meeting, CERN (2013).

[25] G. Dôme, "The SPS acceleration system travelling wave drift-tube structure for the CERN SPS", CERN-SPS-ARF-77-11.

[26] T. Bohl, "The 200 MHz Travelling Wave Cavities in the SPS", Proceedings of the 10th Chamonix SPS and LEP Performance workshop, Chamonix, France (2000).

[27] E. Shaposhnikova *et al.*, "Upgrade of the 200 MHZ RF System in the CERN SPS", CERN-ATS-2011-042.

[28] G. Arduini *et al.*, "Beam observations with electron cloud in the CERN PS and SPS complex", Proceedings of the ECLOUD04 workshop, Napa, CA, USA (2005).

[29] H. Bartosik *et al.*, "Electron Cloud and Scrubbing Studies for the SPS in 2012", CERN-ATS-Note-2013-019 MD.

[30] G. Iadarola *et al.*, "Recent electron cloud studies in the SPS", CERN-ACC-2013-0115.

[31] C. Vallgren *et al.*, "Amorphous carbon coatings for the mitigation of electron cloud in the CERN Super Proton Synchrotron", Phys. Rev. ST Accel. Beams, 14, 071001 (2011).